Ocean-Land-Atmosphere Research
A SCIENCE PARTNER JOURNAL

RESEARCH ARTICLE

Components of the CO_2 Exchange in a Southeastern USA Salt Marsh

James T. Morris[1*] and Gary J. Whiting[2]

[1]Department of Biological Sciences and Belle Baruch Institute for Marine and Coastal Sciences, University of South Carolina, Columbia, SC 29208, USA. [2]Department of Organismal and Environmental Biology, Christopher Newport University, Newport News, VA 23606, USA.

*Address correspondence to: jtmorris@baruch.sc.edu

Different CO_2 exchange pathways were monitored for a year in short- and tall-form *Spartina alterniflora* grasses in a southeastern USA salt marsh at North Inlet, South Carolina. The tall form of grass growing close to a creek under favorable conditions reached a higher standing biomass than the short form of grass growing in the interior marsh. However, the photosynthetic parameters of both forms of grass were equivalent. The tall canopy had greater net canopy production, 973 versus 571 g C m^{-2} $year^{-1}$, canopy growth, 700 versus 131 g C m^{-2} $year^{-1}$, and canopy respiration, 792 versus 225 g C m^{-2} $year^{-1}$, but lower sediment respiration, 251 versus 392 g C m^{-2} $year^{-1}$. In a single growing season, tall-canopy biomass increased to intercept all the available solar radiation, which limits gross photosynthesis. Total respiration increased during the growing season in proportion to live biomass to a level that limited net production. Theoretically, the difference between net canopy production and canopy growth is carbon allocated to belowground growth and respiration. However, the computation of belowground production by this method was unrealistically low. This is important because carbon sequestration is proportional to belowground production and accounts for most of the vertical elevation gain of the marsh surface. Based on the allometry of standing live biomass, alternative estimates of belowground production were 927 and 193 g C m^{-2} $year^{-1}$ in creekbank and interior marshes, which would yield gains in surface elevation of 0.2 and 0.04 cm/year, respectively.

Citation: Morris JT, Whiting GJ. Components of the CO_2 Exchange in a Southeastern USA Salt Marsh. *OceanLand-Atmos. Res.* 2024;3:Article 0077. https://doi.org/10.34133/olar.0077

Submitted 21 May 2024
Revised 19 November 2024
Accepted 19 November 2024
Published 11 December 2024

Introduction

The fixation of CO_2 in any autotrophic ecosystem is limited ultimately by the availability of incident light energy. Odum [1] posited in his theory of ecosystem development that the quotient of gross primary production to respiration approaches unity as an ecosystem matures and approaches maximum biomass. Respiration is proportional to biomass, while gross photosynthesis reaches an asymptotic level as the absorption of photosynthetically active radiation (PAR) by the plant canopy approaches 100%. Consequently, in the early stages, the quotient of gross photosynthesis to biomass is high, and in the mature stages, it is low.

In forests, the time scale of development is decades. In mature, temperate salt marshes, the time scale is months from the time of emergence in the spring to maturity in the autumn. This is supported by measurements of light penetration in the canopies of the salt marsh grass, *Spartina alterniflora*, and CO_2 exchange in a Danish marsh dominated by a community of *Spartina anglica* [2] . A study of light penetration demonstrated that 95% of incident light should be intercepted by a canopy biomass of 1,500 g/m^2 and a corresponding leaf area index (LAI) of 3.2 [3]. This amount of standing live and dead biomass and greater is typical of the more productive stands of *S. alterniflora* found along creekbanks.

The purpose of the present study was to measure the seasonal fluxes of CO_2 in a southeastern USA salt marsh to determine the magnitudes of sources and sinks and to determine if the theory of ecosystem development applies to a salt marsh. A *S. alterniflora* marsh exhibits a wide range of canopy sizes during the growing season, which allows quantifying and modeling relationships between canopy weight, gross photosynthesis, and respiration at various times during the seasonal growth cycle. To accomplish this, we made monthly measurements of CO_2 exchange in short- and tall-form canopies using closed chambers. We measured the drawdown of CO_2 in the light and the production of CO_2 in situ in darkened chambers. The instantaneous rate of gross photosynthesis was calculated as the drawdown rate plus the absolute rate of total chamber respiration. Leaf respiration was calculated by subtracting soil respiration from chamber respiration using in situ incubations of core tubes. The instantaneous rates were numerically integrated using models of photosynthesis and respiration. The results show the seasonality and magnitude of the components of CO_2 exchange in a salt marsh ecosystem and explain the limits of marsh primary production.

Methods

Gas exchange

Monthly photosynthesis and respiration rates were measured for 13 months near the creekbank (tall *S. alterniflora* zone) and interior marsh (higher elevation, short *Spartina* zone) within the Oyster Landing area of the North Inlet salt marsh, South Carolina, USA. Triplicate in situ temperature-controlled, closed chambers at each of the two sites described by Whiting and Morris [4], constructed of clear Plexiglas covering a marsh surface area of 930 cm^2 with varying chamber heights of 30 to 90 cm (depending on vegetation zone), were deployed during low tide to measure CO_2 gas exchange.

Chamber temperatures were regulated within ±1 °C of ambient air temperature by passing chilled water through copper coils mounted at a 30° angle beneath a mixing fan (mounted on top of the chamber). The temperature was controlled by a manual valve regulating the flow of cold water through the coils pumped from an ice–water reservoir. Temperature and ambient PAR were monitored with Hg thermometers and a LI-COR quantum sensor (LI-COR Environmental Division, Lincoln, NE, USA), respectively.

Monthly measurements of net CO_2 uptake (photosynthesis), referred to by Boote et al. [5] as apparent canopy photosynthesis (ACP), were made under full-sunlight conditions (near solar noon) by sampling headspace gas every 10 min for an hour using 10 cm^3 glass syringes (B-D Glaspak, Rutherford, NJ) fitted with 3-way valves (Medex, Hillard, OH). Total chamber respiration (R_T) was measured immediately after by placing an opaque shroud over the chambers to exclude light. Sampling proceeded by sampling the headspace gas every 10 min for an hour. Linear regressions were fitted to the time series of CO_2 concentrations in light and dark to compute the rates of ACP and total chamber respiration (R_T). Gross canopy integrated rate of $CP_{h,t\ is}$ is referred to as total canopy photo-$_{h,t}$ $_T$ photosynthesis was computed as $CP = ACP + R$. The synthesis (TCP).

Net canopy photosynthesis (NCP) was estimated by removing the soil component of CO_2 efflux from ACP. Soil respiration (R_S) was measured alongside the closed chambers using four aluminum core tubes (60 cm length × 10 cm diameter) placed on bare soil between plant stems in each zone (each tube covering an area of 78 cm^2). The core tubes were inserted 30 cm into the sediment with minimal compaction before sampling. At 20-min intervals, the 2.5-l headspace was mixed with a 60-ml syringe before taking a 10-ml sample. A total of 6 gas samples were taken over 2 h. The soil cores did not account for microbial respiration from standing dead biomass, which was accounted for in total chamber respiration (R_T).

Gas samples were analyzed within 24 h on a Carle AGC gas chromatograph equipped with a 6-port sampling valve fitted with a 1-ml gas sampling loop standardized by calibration gas in units of ppmv at STP. The instantaneous rates of $CO^{-}{}_2$ exchange are expressed in units of ml CO_2 m h^{-1}, consistent with the

^{2}

units of the gas standards. Model-integrated rates of CO^{-2} $year^{-1}$. $_2$ exchange are expressed as g C m

Biomass

After each dark series of gas samples, the total standing plant biomass was harvested within each chamber. The harvested biomass was separated into standing live and dead fractions and then dried (70 °C) and weighed.

Models

Total instantaneous canopy photosynthesis ($CP_{h,t}$) was computed using a model of photosynthesis that was derived by integrating two equations over canopy depth (z), one describing the distribution of PAR within the canopy [3] :

$$L_z = L_o e^{-\alpha B_z / \sin\beta} \quad (1)$$

and one that describes the dependence of the leaf-specific rate of photosynthesis on PAR:

$$P_z = f\,[L_z/(L_z+K_L)] \quad (2)$$

L_z and L_o are the PAR at depth z in the canopy and incident at the top of the canopy, B_z is the canopy biomass between the top and depth z, α is the light extinction coefficient, β is the elevation of the sun (Fig. S1), and K_L is the half-saturation constant or level of PAR at which the rate of photosynthesis is half its maximum.

P_z was integrated analytically over canopy depth z after substituting for L_z from Eq. 1 to give an equation that represents the total instantaneous rate of gross canopy photosynthesis (ml CO_2 m^{-2} h^{-1}) on day t and hour h [2]:

$$CP_{h,t} = [c_1 + c_2 \sin(2\pi t/365 + c_3)] \times q \times \sin\beta \times \left[\ln(L_o + K_L) - \ln\left(L_o e^{-\frac{\alpha B_C}{\sin\beta}} + K_L \right) \right] / \alpha \quad (3)$$

Independent variables in the model are the live canopy biomass (B_c), the incident light (L_o)as PAR normal to the beam of light, the angle of the sun b, the green fraction of the canopy (q), and the day of the year (t). A version of the model referred to as the round, green canopy model with ^{2}), and $\sin\beta$ = 1 was the best fit. The interpretation q = 1, B_C = live biomass (g/m

of this variant is that green leaves tend not to be shaded by dead leaves and the canopy is equally efficient at absorbing the incident light at any solar elevation, i.e., the canopy is like a collection of randomly oriented green leaves. Parameter values in the model were obtained by fitting the model equations by nonlinear regression [6] to the instantaneous

rates of gas exchange (ACP + R_T). E quation 3 was integrated numerically (E q. 4) to give daily and hourly rates of total gross canopy photosynthesis using a model coded in Fortran.

$$TCPCP_{h,t} = \int_{t=1}^{365} \int_{h=1}^{24} \quad (4)$$

The instantaneous weight-specific rate of leaf respiration (R_L) (ml CO_2 m^{-2} h^{-1}) was modeled as a seasonally variable function of the Arrhenius equation [7]:

$$R_L = [m_L + a_L \sin(2\pi t/365 + p_L)] e^{A_L/T} \quad (5)$$

where constants are m_L, the annual mean, a_L, the seasonal amplitude, p_L, the phase shift that sets the time of maximum respiration modified by temperature, the natural base e, and A_L . Variables are t, the ordinal day (1 to 365), and air temperature T (°C). Leaf respiration measured in the chambers included an unknown amount of microbial respiration on standing dead biomass that was not accounted for by the core estimates of soil respiration.

Soil respiration (R_S) (ml CO_2 m^{-2} h^{-1}) was best described by a simple harmonic where m_s is the annual mean respiration, a_s is the seasonal amplitude, t is the ordinal day (1 to 365), and p_s is the phase shift that sets the time of minimum and maximum soil respiration:

$$R_S = [m_s + a_s \sin(2\pi t/365 + p_s)] \quad (6)$$

Results

Site differences

The tall- and short-form sites differed in several important metrics including maximum live standing biomass, belowground biomass, and elevation. Mean tall-form biomass was form biomass was greatest in July and averaged 511 greatest during September, 2,027 ± 355 g/m^2 (±1 SD). Short-± 67 g/m_2

(Table S1). An RTK survey in 2021 found average site elevations of 0.46 ± 0.03 m (± 1 SD) and 0.23 ± 0.1 m (NAVD88) in the short-canopy, interior-marsh zone and tall-canopy, lowmarsh zone.

Gross canopy photosynthesis ($CP_{h,t}$)

The canopy-depth integrated rate of photosynthesis varied from nearly zero during winter to a maximum of about 2,300 ml CO^{-2} h^{-1} during the late summer months. The photosynthetic $_2$

m

Leaf respiration (R_L)

At constant temperature, weight-specific (live weight) canopy respiration (R_L) was greatest during early spring (early March, Fig. 3) when standing biomass was low, and was approximately twice as great in the tall canopy than in the short. However, by late in the growing season when standing biomass was greatest, R_L in both sites had converged to a low level (Fig. 3) . The empirical rates varied seasonally in the short canopy from 0.11 ± 0.07 to 1.03 ± 0.3 (±1 SD) and from 0.12 ± 0.04 to 1.5 ± 0.3 ml CO_2 g^{-1} h^{-1} in the tall canopy.

Soil respiration (R_S)

Soil respiration peaked in early July (Fig. 4) and followed approximately the seasonal temperature cycle (Fig. S2). It was significantly greater in the interior marsh (short canopy) than in the tall-canopy site [8] . The interior-marsh site had soil respiration that varied seasonally from 14 $^{-1}$ h^{-1} in July, while respiration in the tall-canopy site varied ± 4 in January to 236 ± 10 ml CO_2

g from 10 ± 4 to 116 ± 85 ml CO_2 g^{-1} h^{-1}.

parameters of the gross photosynthesis model (Eq. 3) did not differ between tall- and short-form canopies, and a single set of coefficient values explained 90% of the variation in rates in both canopy types (Fig. 1). The value of parameter c_3 (5.75 radians) implies that for a constant level of PAR, the maximum weightspecific photosynthetic rate occurred in early May. With the PAR constant, the photosynthetic rate varied from a high of 10 ($^{-1}$ h^{-1} (per live dry weight). $c_1 + c_2$) to a low of 4.3 ml CO_2 g

When the observed and model-calculated rates (Eq. 3) were plotted against standing biomass by month, gross photosynthesis was seen to approach asymptotic levels in late summer (Fig. 2) . This was especially true of the tall-form canopies because their standing biomass was greater than the short-form canopy. By

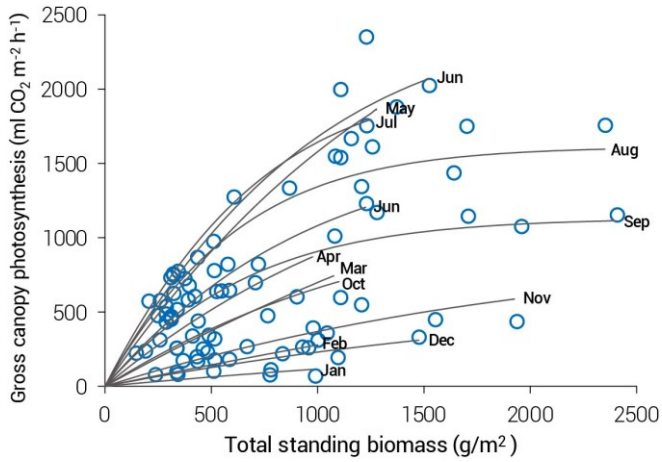

Fig. 2. Observed rates of gross canopy photosynthesis (o) per marsh surface area (ACP+ R_T) and rates calculated from the canopy photosynthesis model (—) shown as a function of total standing biomass. Rates are shown for different months.

June, the tall-form canopy had reached a live weight of 747 $^{-2}$ h^2 and gross canopy photosynthesis of 1,855 $^{-1}$, and by August, the live weight had increased to ± 179 ml ± 141 g m

11CO,646 ,686 $_2$ m±± 183 ml CO 320 g m^{-2} and gross photosynthesis had decreased to $_2$ m^{-2} h^{-1}.

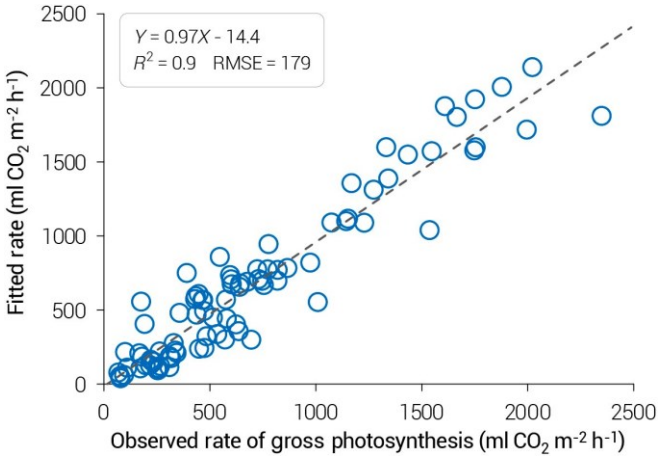

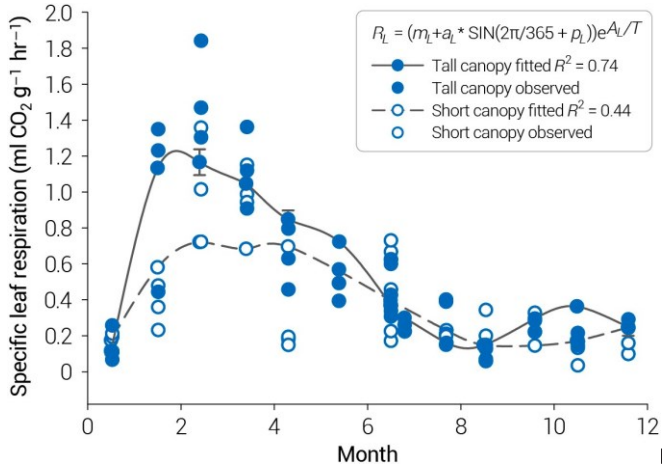

Fig. 1.

Regression of the fitted against the observed rates of canopy gross photosynthesis.

Rates of gross photosynthesis (per marsh surface area) were measured during each of Fig. 3. Observed and fitted rates of weight-specific leaf respiration (per live weight) 12 consecutive months at various levels of biomass in both short and tall canopies (n = 6). by site and month. For the short canopy, m_L = 0.69, a_L = 0.5, p_L = −0.02, and A_L = The best fit returned parameters c_1 = 7.12, c_2 = 2.8, c_3 = 5.75, K_L = 1,561.5, and α = 0.0026. −10.1. For the tall canopy, m_L = 1.59, a_L = 1.34, p_L = 0.47, and A_L = −19.0.

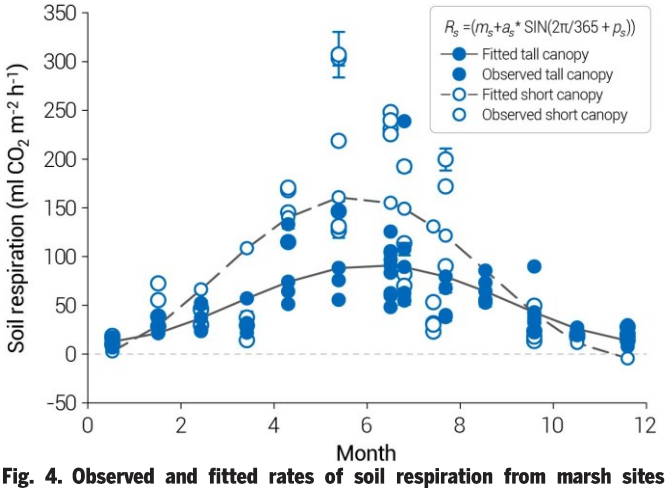

Fig. 4. Observed and fitted rates of soil respiration from marsh sites supporting short and tall *S. alterniflora* canopies. Soil respiration differed between sites at the $P = 0.01$ level according to Tukey's multiple comparison test. For the short canopy, $m_s = 78.7$, $a_s = 83.4$, and $p_s = 4.8$, $r^2 = 0.55$; for the tall canopy, $m_s = 51.7$, $a_s = -39.7$, and $p_s = 4.6$, $r^2 = 0.44$.

Total chamber respiration (R_T)

One of the checks and balances used to assess the overall model was a regression of the predicted total chamber respiration, computed as the sum of predicted total leaf ($B_C R_L$) and soil respiration (R_S), against the observed total chamber respiration (Fig. 5). The linear fit accounted for 70% of the variation. The greatest variation was at the highest total respiration rates in tall-canopy sites.

Net canopy photosynthesis

The models of gross canopy photosynthesis and total leaf respiration (Eqs. 3 and 4) were solved to compute net rates of canopy photosynthesis (NCP = TCP − $B_C R_L$) for the observed ranges of canopy biomass in tall- and short-canopy types on several dates from June to October (Fig. 6). Both canopy types show diminishing returns to scale for biomass, and nearly the same rates on each date, except that growth of the short canopies terminated at smaller canopy biomass at an earlier time of year. That is, the short and tall canopies had similar weightspecific rates of net photosynthesis. Yet, the tall canopy grew to a greater biomass than the short canopy.

Live fraction of canopy biomass

One possible explanation for the difference in canopy growth between sites could be the fraction of the canopy that is senescent or dying (Fig. 7). Leaf growth is compounded. If the short canopy senesced at a faster rate than the tall canopy, then total canopy growth would be lower. However, this was not the case statistically as determined by an analysis of variance (SAS PROC GLM), although the coefficients in the harmonic models differed slightly (Fig. 7).

The seasonal components of CO_2 exchange

The annual integrated rate of NCP was 973 g C m^{-2} $year^{-1}$ in the tall canopy and 571 g C m^{-2} $year^{-1}$ in the short canopy

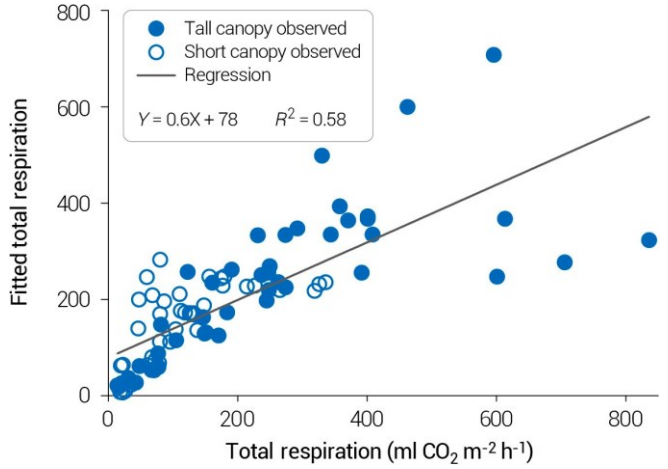

(Table 1). Tall-canopy growth (September maximum–March minimum) of standing biomass (living and dead) was 700 ^{2} $year^{-1}$ (±1 SD) after converting from dry weight, ± 282 g C m while the short-canopy growth of standing biomass was 131 ±

Fig. 5. Total respiration computed as $R_T = R_S + B_C R_L$. Soil respiration (R_S) is shown in Fig. 4, and weight-specific leaf respiration (R_L) is shown in Fig. 3. Standing live biomass is B_C.

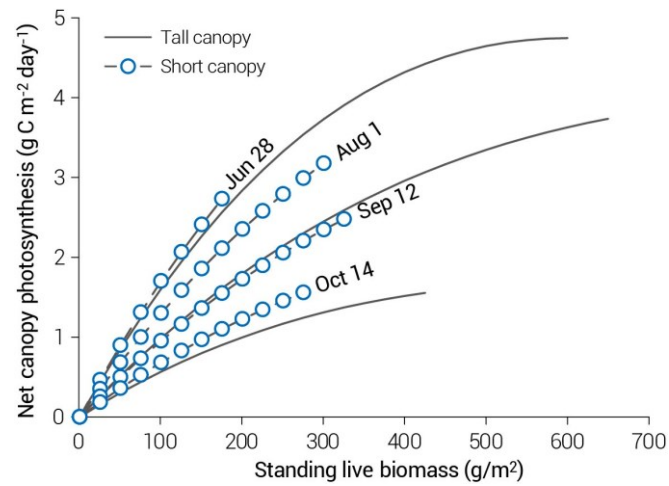

Fig. 6. Model-calculated net canopy photosynthesis (NCP = TCP − $B_C R_L$) versus standing live biomass for select times of year. Curves extend to the maximum live biomass harvested from the chambers at the indicated time of year.

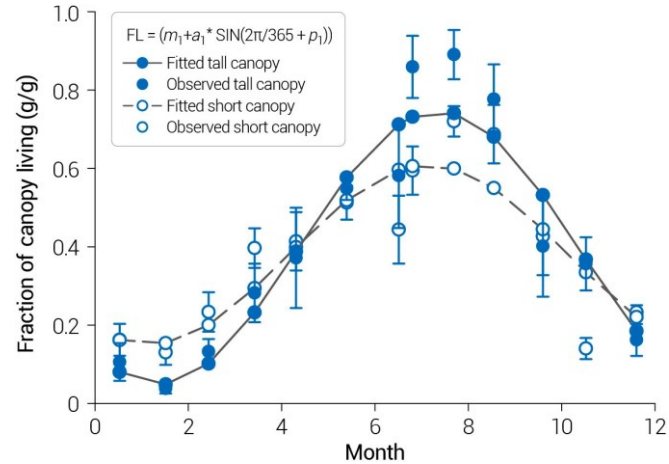

Fig. 7. The fraction of biomass living in short- and tall-form *S. alterniflora* canopies. The harmonic regressions returned R^2 values of 0.67 and 0.84 for the short- and tall-form canopies, respectively. Neither site (short versus tall) nor day–site interactions were significant (SAS PROC GLM). Model coefficients were $m_1 = 0.38$, $a_1 = 0.23$, and $p_1 = 180$ for the short canopy and $m_1 = 0.4$, $a_1 = 0.35$, and $p_1 = 180$ for the tall canopy.

Table 1. Derivative CO_2 exchange calculations

	Tall canopy	Short canopy	Units
a) NCP (Table 3)	973	571	g C m^{-2} $year^{-1}$
b) Canopy growth [a]	700.1 ± 281.9	130.8 ± 63.6	g C m^{-2} $year^{-1}$
c) Available for BG growth and BG respiration (a - b)	273	440	g C m^{-2} $year^{-1}$
d) Sediment respiration (Table 3)	251	392	g C m^{-2} $year^{-1}$
e) Net belowground production (c - d)	22	48	g C m^{-2} $year^{-1}$

[a]Maximum–minimum biomass (+1 SD) from Table S1 and converted to carbon using a conversion factor of 0.55 [31]

64 g C m^2 $year^{-1}$ (July maximum–March minimum) (Table S1). The carbon available for translocation to roots and rhizomes was conservatively estimated as net canopy production NCP minus canopy growth or 973 − 700 = 273 and 571 − 131 = 440 g C m^{-2} $year^{-1}$ in the tall and short canopies, respectively (Table 1). This is consistent qualitatively with the annualized rates of sediment carbon emissions of 251 and 392 g C m^2 $year^{-1}$ in tall and short canopies, respectively (Table S1), and with belowground biomass at these sites, estimated to be 2,400 and 4,870 g dry wt m^{-2} of necromass, and 99 and 219 g dry wt m^{-2} of live belowground biomass in tall and short zones, respectively [9]. The live biomass in the tall zone was unrealistically low considering the canopy biomass (Table 2) .

Discussion

The model of CP (Eq. 3) described both short and tall canopies equally well with one set of constants, i.e., at the same biomass, both canopy types had equivalent rates of TCP (Fig. 1) , although the short *S. alterniflora* canopy never reached a standing biomass equal to the tall canopy. This suggests that short-canopy plants allocated a greater proportion of fixed carbon to roots and rhizomes (Table 1 E). Leaf growth is compounded, and even a small difference in allocation between leaves and roots or rhizomes can have a major impact on total production. The differences in edaphic conditions might account for this dichotomy [10 – 14]. The tall form of *S. alterniflora* grows at a lower elevation, close to or on creek banks where drainage is better, and salinity is usually lower and less variable than the higher elevation zone that supports the short form of *S. alterniflora* in the interior marsh. This interpretation is consistent with measurements of the belowground biomass [8 , 9] that show that the short canopy had a higher root biomass. It is also consistent with measured soil respiration, which was greater on sites supporting the short form of *Spartina* than on sites supporting the tall form of grass (Fig. 4). However, the lower soil respiration near the creekbanks may be a result of greater drainage and loss of dissolved inorganic carbon (DIC) [8].

Table 2. Alternative calculations of belowground production based on empirical allometric ratios [15] and functional balance theory [17]

	Tall canopy	Short canopy	Units
a) Net belowground production [a]	1,686	350	g dry wt m^{-2} $year^{-1}$
b) Lignin content [32]	0.1	0.1	g/g
c) Organic accretion (a × b)	169	35	g dry wt m^{-2} $year^{-1}$
d) Organic selfpacking density [21]	0.085	0.085	g/cm^3
e) Contribution to vertical accretion (10^{-4} × c/d)	0.2	0.04	cm/year

[a]Assumed to be equivalent to maximum live standing biomass (Table S1) based on the logic that root and leaf production are balanced, while rhizomes are perennial and turnover slowly.

There are alternative interpretations of the differential partitioning hypothesis. One is that leaf senescence is greater in the short canopy, although this was not supported by the empirical data (Fig. 7) . A second possibility is that losses of dissolved organic carbon (DOC) and DIC were proportionally greater near the creekbank than the interior marsh. Losses of DOC and DIC were not accounted for, but an earlier estimate placed the potential loss of DIC from the creekbank area at 175 g C m^{-2} $year^{-1}$ [4], which is 70% of the sediment respiration (Table 1).

In theory, the net growth of roots and rhizomes would equal the allocation of fixed carbon to roots and rhizomes (Table 1 C) minus belowground respiration (Table 1 D), assuming no losses of DOC or DIC. Therefore, the CO_2 exchange rates indicate that the net production of roots and rhizomes in the tall and short canopies could be only 22 and 48 g C m^2 $year^{-1}$. These greatly underestimate belowground production [1 5] . The ratios of belowground to canopy growth must be much greater than 22/700 and 48/131. Based on a simple allometric assumption that leaf growth and root growth are balanced, belowground production should be about 1,686 and 350 g C m^{-2} $year^{-1}$ in the tall and short forms of canopies, respectively (Table 2). The allometric ratio is based on work by Brenchley [16] and others that show that the activity of leaves is proportional to the total root activity, and this determines the root:shoot ratio. The nitrogen uptake rate by *S. alterniflora* at high availability coupled with high photosynthetic rates results in a ratio of roots:leaves (rhizomes excluded) of about 1:1 [15

, 17]. Therefore, it is most likely that the CO_2 exchange-based estimate of carbon allocation to roots and rhizomes in both tall and short canopies was greatly underestimated by the CO_2 exchange calculations.

The feasibility of the belowground production rate can be assessed by computing its contribution to the rate of elevation gain of the marsh surface (Table 2 E). Based on a lignin concentration of about 10% [1 5, 18– 20] , in a steady state, the tall and short canopies should sequester about 169 and 35 g dry wt m^{-2} $year^{-1}$. Dividing by the self-packing density of sediment organic matter, 0.085 $g/cm^3 \times 10^4$ cm/m^2 [21], gives vertical accretion rates of 0.2 and 0.04 cm/year, which are reasonably consistent with measured accretion rates in similar areas in North Inlet of 0.28 and 0.11 cm/year [1 5] considering variability in productivity and lignin.

What can account for the missing carbon in the CO_2 exchange calculations? It cannot be caused by chemoautotrophy or sulfide oxidation in the roots or rhizosphere. Any sulfide production by sulfate-reducing bacteria depends directly or indirectly on organic substrates produced by plants and so must be accounted for by photosynthesis. One potential source of unaccounted carbon fixation is from CO_2 diffusing into the plant's aerenchyma from the sediment. This was estimated by measuring the CO_2(g) flow from the cut ends of *S. alterniflora* stems [8] . The rates depended on stem diameter, averaging 82 and 108 µl CO_2 min^{-1} in short- and tall-canopy sites, respectively. Based on stem densities and extrapolating to the growing season, the potential diffusion rates were 148 and 194 g C m^{-2} $year^{-1}$. This is likely an overestimate because the method of flowing N_2 gas over the cut culms and trapping the CO_2 increased the diffusion gradient, and in the unlikely event that the plants could fix carbon at this rate, the addition to total gross photosynthesis would only be 11 to 19%. Nevertheless, the volume percent concentration of CO_2 in the aerenchyma is several percent [22], which raises a question about the possibility of its use by the plant. It is a mystery how the plant can pull CO_2 from the atmosphere against such a steep gradient unless the gas transport system is isolated from the chlorophyll. Any escape of internal CO_2 to the atmosphere would contribute to the measured leaf respiration and decrease the calculated rate of carbon available to belowground production.

In a mature marsh, the tall form of *S. alterniflora* routinely reaches a biomass that approaches the limits of total gross photosynthesis. Its canopy reaches a biomass capable of intercepting all the available light because of self-shading. The short canopy does not reach this level of standing biomass. From measurements of the vertical distribution of sunlight in *Spartina* canopies, it was estimated that 95% of incident noon light was intercepted by a canopy of 1,500 g/m^2 with a corresponding leaf area index of 3.2 [3] . Furthermore, the mean of measured light extinction coefficients was 0.002 compared to the α of 0.0026 as determined by a fit of the canopy photosynthesis model (Eq. 3 and Fig. 1) .

This study has implications for blue carbon and resilience to rising sea level. The accumulation of organic matter in marsh sediment is limited by primary productivity and by the creation of accommodation space caused by rising sea level. There is a maximum rate of productivity, which is determined by photosynthetic efficiency, solar radiation, and the rate of sea-level rise (SLR). If SLR is too low, the marsh elevation will rise to the upper vertical limit and productivity will approach zero. If SLR exceeds the capacity of the marsh to accumulate organic and mineral sediment, elevation will decrease to the lower vertical limit of plant growth.

The chamber-based CO_2 exchange calculations have several problems such as the lack of accounting of DOC and DIC losses. The chamber incubations also did not account for advective fluxes of CO_2 out of the sediment during a rising tide, although these were only 10% of the diffusive flux [23]. Another potential problem is the effect of tidal flooding on atmospheric exchange. Eddy flux measurements have shown that net ecosystem exchange (NEE) during marsh flooding was inversely proportional to flood depth and duration [24]. The tides at our sites rarely overtop the canopy, and the average flood duration is less than 30% of the time. Moreover, partial flooding may have a greater effect on light attenuation than gas exchange because the leaf surface of *Spartina* is corrugated and hydrophobic, which allows for the conduction of gases through the external air layers. In *Oryza*, CO_2 diffuses from the surrounding water into the leaf in daylight, while O_2, which has limited solubility in water, is expelled through the air layers into the atmosphere, provided that some part of the leaf is subaerial. At night, air is conducted from the atmosphere through the air layers along a pressure gradient created by the solubilization in water of respiratory CO_2 [25].

Eddy covariance methods are subject to some of these same problems but do provide continuous, spatially integrated measurements of net CO_2 exchange. Commonly referred to as NEE, and conceptually equivalent to ACP, neither method can account for losses of DIC and DOC. A major advantage of the eddy covariance method is the length of time series measurements, often spanning multiple years. A significant finding has been the magnitude of variability of annual rates, which can be attributed to environmental variables. Forbrich et al. [26] measured rates of 104 to 233 g C m^{-2} $year^{-1}$ (our convention is to treat uptake as positive) in a New England salt marsh and attributed the variation to changes in rainfall early in the growing season. Considering the short growing season, these rates compare favorably to our estimates of ACP of 179 and 722 g C m^{-2} $year^{-1}$ (Fig. 8 and Table 3). Chu et al. [27] measured NEE by eddy covariance over 8 years in a Yellow River Delta marsh, China of 8 to 85 g C m^{-2} $year^{-1}$ and also attributed the variability to early season precipitation. A NEE of 286 g C m^{-2} $year^{-1}$ was reported in a *Spartina densiflora* marsh [28] . One of the highest rates of NEE (387 g C m^{-2} $year^{-1}$) was reported for a newly planted marsh (2011) in the San Francisco Bay [29]. The high net uptake of CO^{-1}_2) was attributed to low respiration emissions (498 g C m, which were probably due to the youthful age of the $^{-2}$

year

marsh. One outlying study [30] found a Delaware salt marsh to be a net source of carbon to the atmosphere, losing a net of 222 g C m^{-2} $year^{-1}$ from a total respiration of 1,646 g C m^{-2} $year^{-1}$. We conclude from these studies that variability in net CO_2 exchange is due to climate, marsh age,

physiography, and the partitioning of losses among CO_2(g), carbon sequestration, DIC, and DOC.

Conclusion

Exchanges of CO_2 between a southeastern salt marsh and the atmosphere were measured monthly using static chambers in areas dominated by the short and tall form of *S. alterniflora*. The chamber measurements were integrated using models of photosynthesis and respiration that accounted for hourly and seasonal changes in air temperature and incident PAR. ACP was 722 and 179 g C m^{-2} $year^{-1}$ in the tall and short canopies. Total respiration in the tall canopy was dominated by canopy respiration, which amounted to 792 g C m^{-2} $year^{-1}$ or 76% of the total, while soil respiration of 392 g C m^{-2} $year^{-1}$, 64% of the total, dominated in the short canopy (Table 3). Soil respiration, not accounting for losses of DIC, was lower in sites supporting the tall form of *Spartina*, 251 g C m^{-2} $year^{-1}$, and correlated with belowground biomass from soil cores [8 , 9]. Leaf growth, estimated by maximum–minimum, was greater in the tall canopy than in the short canopy or 700 versus 131 g C m^{-2} $year^{-1}$(Table 1). Primary production allocated to roots and rhizomes or gross belowground production was calculated by

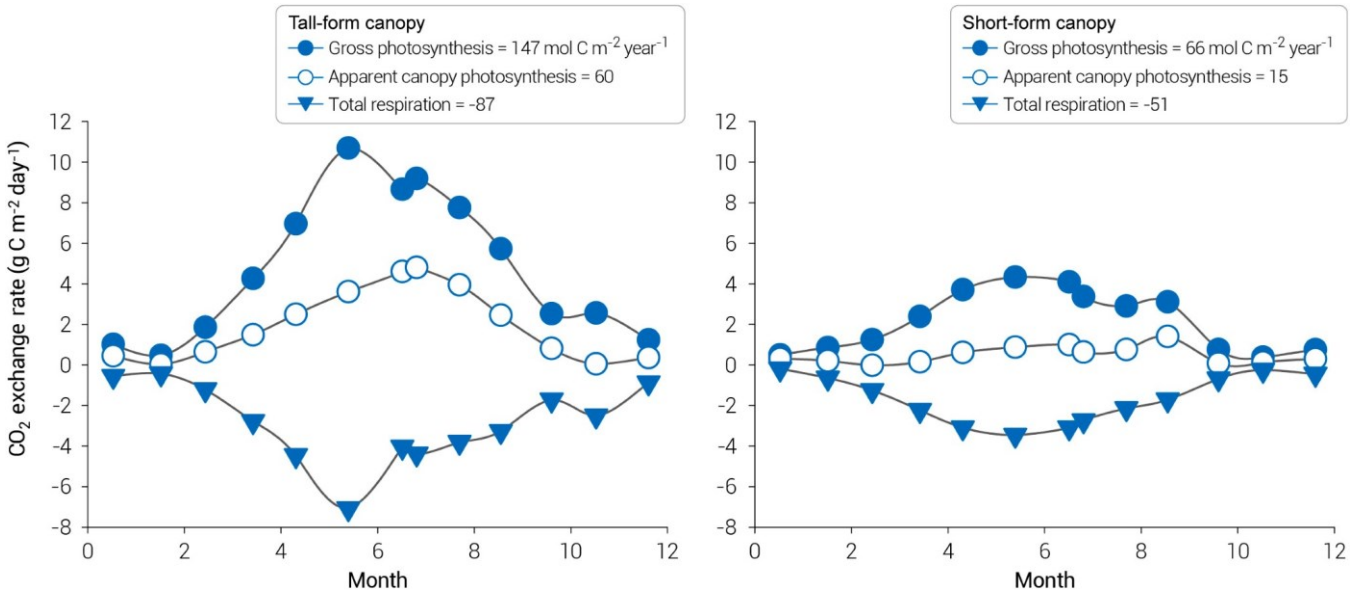

Fig. 8. Daily integrated rates of gross canopy photosynthesis (TCP), total respiration ($R_T = -B_CR_L - R_S$), and apparent canopy photosynthesis (ACP = TCP − $|R_T|$) by month and site. Also shown in the legends are the annual integrated rates.

Table 3. Model-integrated rates of daily CO_2 exchange (g C m^{-2} d^{-1}) in tall and short *S. alterniflora* zones by month. Total canopy photosynthesis (TCP) was computed as the hourly rate of CO_2 drawdown under full sun [apparent canopy photosynthesis (ACP)] after adding back total chamber respiration (R_T). Total chamber respiration (R_T) was decomposed into soil (R_S) and canopy respiration (B_CR_L). Net canopy production (NCP) was computed as TCP − B_CR_L, and ACP as NCP − R_S. Daily rates were made by integrating the model Eqs. 3 to 5 (see text) over 24 h while accounting for hourly changes in temperature and photosynthetically active radiation (PAR). PAR was from the computed solar elevation angle [33]. Temperature was computed from a harmonic analysis of measured hourly temperatures. Shown are air temperatures at the times chambers were operated and hours of daylight on the days that chambers were operated.

		Daylight hours	Tall canopy					Short canopy				
Month	Temperature (°C)		TCP	B_CR_L	NCP	R_S	ACP	TCP	B_CR_L	NCP	R_S	ACP
0.5	7.3	11	1.00	0.40	0.61	0.16	0.44	0.491	0.16	0.33	0.03	0.30
1.5	7.9	11	0.46	0.16	0.31	0.28	0.03	0.85	0S27	0.58	0.38	0.20
2 .4	10.3	11	1.85	0.74	1.11	0.48	0.64	1.239	0.41	0.83	0.85	–0.02
3 .4	14.3	13	4.26	2.05	2.21	0.73	1.48	2.388	0.84	1.55	1.40	0.15
4.3	18.2	13	6.96	3.51	3.45	0.95	2.50	3.704	1.29	2.42	1.80	0.61
5 .4	22.3	15	10.69	5.94	4.75	1.14	3.61	4.331	1.39	2.94	2.07	0.87
6.5	24.4	13	8.66	2.88	5.77	1.17	4.61	4.09	1.10	2.99	1.99	0.99
6.8	24.5	13	9.19	3.24	5.95	1.15	4.80	3.37	0.83	2.54	1.92	0.63
7.7	23.5	13	7.75	2.79	4.97	1.02	3.95	2.902	0.59	2.31	1.56	0.75
8 .5	21.0	13	5.72	2.45	3.28	0.83	2.45	3.113	0.61	2.50	1.11	1.40
9.6	16.6	11	2.53	1.17	1.35	0.55	0.80	0.755	0.15	0.61	0.54	0.07
10.5	12.5	11	2.56	2.18	0.38	0.33	0.05	0.372	0.11	0.26	0.15	0.12
11.6	8.8	9	1.23	0.70	0.53	0.18	0.35	0.744	0.28	0.47	0.18	0.29
Annualized (g C m^{-2} $year^{-1}$)			1,765	792.1	973	251	722	796	225	571	392	179

subtracting leaf respiration and growth from gross photosynthesis, which gave 273 and 440 g C m^{-2} $year^{-1}$ for the tall and short zones, respectively. The photosynthetic parameters in both canopy types were equivalent, suggesting that the difference in canopy growth was due to differences in the allocation of photosynthate to roots and rhizomes, which was proportionally greater in the short canopy. However, net belowground production from the CO_2 exchange calculations was

unrealistically low, and there is an unaccounted, missing piece of the carbon budget.

Acknowledgments

Funding: This work was funded by NSF awards 2203324 and 1654853.

Author contributions: Conceptualization: J.T.M. and G.J.W. Methodology: G.J.W. and J.T.M. Funding acquisition: J.T.M. Writing—original draft: J.T.M. Writing—review and editing: J.T.M. and G.J.W. Data acquisition and curation: J.T.M. and G.J.W. **Competing interests:** The authors declare that they have no competing interests.

Data Availability

Raw gas exchange data are available from J.T.M. upon request and in the Supplementary Materials. Meteorological data are available online: https://sc.edu/study/colleges_schools/artsandsciences/baruch_institute/data_publications/meteorological/index.php.

Supplementary Materials

Figs. S1 and S2
Table S1

References

1. Odum EP. The strategy of ecosystem development: An understanding of ecological succession provides a basis for resolving man's conflict with nature. *Science*. 1969;164(3877):262–270.
2. Morris JT, Jensen A. The carbon balance of grazed and nongrazed Spartina anglica saltmarshes at Skallingen, Denmark. *J Ecol*. 1998;86(2):229–242.
3. Morris JT. Modelling light distribution within the canopy of the marsh grass Spartina alternilfora as a function of canopy biomass and solar angle. *Agric For Meteorol*. 1989;46(4):349–361.
4. Whiting GJ, Morris JT. Nitrogen fixation (C2H2 reduction) in a salt marsh: Its relationship to temperature and an evaluation of an in situ chamber technique. *Soil Biol Biochem*. 1986;18(5):515–521.
5. Boote KJ, Bennett JM, Jones JW, Canopy photosynthesis: Apparent, net, or gross? In: Sybesma C, editor. *Advances in photosynthesis research: Proceedings of the VIth International Congress on Photosynthesis, Brussels, Belgium, August 1–6, 1983, Volume 4*. Dordrecht: Springer Netherlands; 1984. p. 121–124.
6. SAS Institute Inc. *SAS/ETS® 922 User's Guide*. Cary (NC): SAS Institute; 2010.
7. Johnson IR, Thornley JHM. Temperature dependence of plant and crop process. *Ann Bot*. 1985;55(1):1–24.
8. Morris JT, Whiting GJ. Emission of gaseous carbon dioxide from salt-marsh sediments and its relation to other carbon losses. *Estuaries*. 1986;9(1):9–19.
9. Whiting GJ. Nitrogen cycling in salt marshes: Tidal and gaseous exchanges [thesis]. [Columbia (SC)]: University of South Carolina; 1985.
10. Shea ML. Photosynthesis and photorespiration in relation to the phenotypic forms of Spartina alterniflora [thesis]. [New Haven (CT)]: Yale University; 1977. p. 59.
11. Mendelssohn IA, Morris JT. Eco-physiological controls on the productivity of *Spartina alterniflora* Loisel. In: Weinstein MP, Kreeger DA, editors. *Concepts and controversies in tidal marsh ecology*. Dordrecht: Springer; 2000. p. 59–80.
12. Mendelssohn IA, Seneca ED. The influence of soil drainage on the growth of salt marsh cordgrass Spartina alterniflora in North Carolina. *Estuar Coast Mar Sci*. 1980;11(1):27–40.
13. King GM, Klug M, Wiegert RG, Chalmers AG. Relation of soil water movement and sulfide concentration to Spartina alterniflora production in a Georgia salt marsh. *Science*. 1982;218(4567):61–63.
14. Howes BL, Dacey JW, Goehringer DD. Factors controlling the growth form of Spartina alterniflora: Feedbacks between above-ground production, sediment oxidation, nitrogen and salinity. *J Ecol*. 1986;74(3):881–898.
15. Morris JT, Sundberg K. Responses of coastal wetlands to rising sea-level revisited: The importance of organic production. *Estuar Coasts*. 2024;47:1735–1749.
16. Brenchley WE. The effect of the concentration of the nutrient solution on the growth of barley and wheat in water cultures. *Ann Bot*. 1916;30(1):77–90.
17. Morris J, Shaffer G, Nyman J. Brinson review: Perspectives on the influence of nutrients on the sustainability of coastal wetlands. *Wetlands*. 2013;33:975–988.
18. Wilson JO. Decomposition of [^{14}C] lignocelluloses of Spartina alterniflora and a comparison with field experiments. *Appl Environ Microbiol*. 1985;49:478.
19. Hodson R, Christian R, Maccubbin A. Lignocellulose and lignin in the salt marsh grass Spartina alterniflora: Initial concentrations and short-term, post-depositional changes in detrital matter. *Mar Biol*. 1984;81:1–7.
20. Buth GJC, Voesenek LACJ. Decomposition of standing and fallen litter of halophytes in a Dutch salt marsh. In: Huiskes AHL, Blom CWPM, Rozema J, editors. *Vegetation between land and sea: Structure and processes*. Dordrecht: Springer Netherlands; 1987. p. 146–162.
21. Morris JT, Barber DC, Callaway JC, Chambers R, Hagen SC, Hopkinson CS, Johnson BJ, Megonigal P, Neubauer SC, Troxler T, et al. Contributions of organic and inorganic matter to sediment volume and accretion in tidal wetlands at steady state. *Earths Future*. 2016;4(4):110–121.
22. Hwang YH, Morris JT. Evidence for hygrometric pressurization in the internal gas space of Spartina alterniflora. *Plant Physiol*. 1991;96(1):166–171.
23. Morris JT, Whiting GJ. Gas advection in sediments of a South Carolina salt marsh. *Mar Ecol Prog Ser*. 1985;27: 187–194.
24. Moffett KB, Wolf A, Berry JA, Gorelick SM. Salt marshatmosphere exchange of energy, water vapor, and carbon dioxide: Effects of tidal flooding and biophysical controls. *Water Resour Res*. 2010;46(10):W10525.
25. Raskin I, Kende H. How does deep water rice solve its aeration problem. *Plant Physiol*. 1983;72(2):447–454.
26. Forbrich I, Giblin A, Hopkinson C. Constraining marsh carbon budgets using long-term C burial and contemporary atmospheric CO_2 fluxes. *J Geophys Res Biogeosci*. 2018;123(3):867–878.

27. Chu X, Han G, Wei S, Xing Q, He W, Sun B, Li X, Hui D, Wu H, Wang X, et al. Seasonal not annual precipitation drives 8-year variability of interannual net CO2 exchange in a salt marsh. *Agric For Meteorol*. 2021;308–309:Article 108557.
28. Tonti NE, Gassmann MI, Pérez CF. First results of energy and mass exchange in a salt marsh on southeastern South America.
Agric For Meteorol. 2018;263:59–68.
29. Shahan J, Chu H, Windham-Myers L, Matsumura M, Carlin J, Eichelmann E, Stuart-Haentjens E,
Bergamaschi B, Nakatsuka K, Sturtevant C, et al. Combining eddy covariance and chamber methods to better constrain CO2 and CH4 fluxes across a heterogeneous restored tidal wetland. *J Geophys Res Biogeosci*. 2022;127(9):e2022JG007112.
30. Hill AC, Vargas R. Methane and carbon dioxide fluxes in a temperate tidal salt marsh: Comparisons between plot and ecosystem measurements. *J Geophys Res Biogeosci*. 2022;127(7):e2022JG006943.
31. Drexler JZ, Fontaine CS, Deverel SJ. The legacy of wetland drainage on the remaining peat in the Sacramento—San Joaquin Delta, California, USA. *Wetlands*. 2009;29:372–386.
32. Morris JT, Callaway JC. Physical and biological regulation of carbon sequestration in tidal marshes. In: Windam-Meyers L, Crooks S, Troxler T, editors. *A blue carbon primer: The state of coastal wetland carbon science, practice, and policy*. Boca Raton
(FL): CRC Press; 2018. p. 67–79.
33. Sellers WD. *Physcial climatology*. Chicago (IL): University of Chicago Press; 1965. p. 272.